

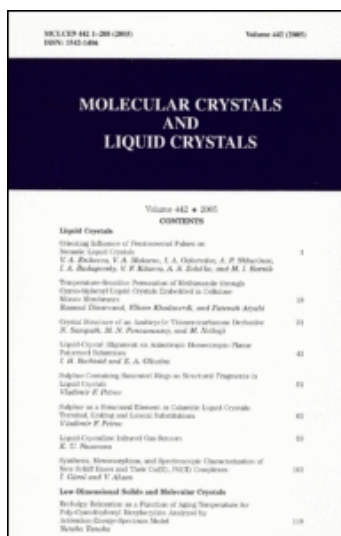
This article was downloaded by: [Barbero, C. A.]

On: 23 July 2010

Access details: Access Details: [subscription number 922646012]

Publisher Taylor & Francis

Informa Ltd Registered in England and Wales Registered Number: 1072954 Registered office: Mortimer House, 37-41 Mortimer Street, London W1T 3JH, UK



MOLECULAR CRYSTALS AND LIQUID CRYSTALS	
Volume 442 • 2005	
CONTENTS	
Liquid Crystals	
Viscosity Behavior of Hexamethyl Polysiloxane as Smectic Liquid Crystals	1
V. A. Barbero, V. R. Miras, J. A. Olivares, A. P. Villarreal, J. A. Rodriguez, V. P. Rivarola, A. A. Zúñiga, and M. C. Miras	
Temperature-Induced Permeation of Polystyrene through Crosslinked Liquid Crystals Embedded in Cellulose Matrix Structures	10
Ronald Dharwadkar, Ekman Khattarwadi, and Patrick Ajayi	
Crystal Structure of an Anisotropic Thermotropic Liquid Crystalline Polymer	21
J. H. Rodriguez and J. A. Olivares	
Liquid Crystal Alignment on Anisotropic Hexamethyl Polysiloxane	41
J. H. Rodriguez and J. A. Olivares	
Substrate Containing Hexamethyl Polysiloxane and Tripropyl in Liquid Crystals	51
Manfred J. Peter	
Substrate as a Structural Element in Columnar Liquid Crystals: Thermal Stability and General Substitutions	61
Manfred J. Peter	
Liquid Crystals: Infrared Gas Sensors	81
M. C. Miras	
Optical, Microscopic, and Spectroscopic Characterization of New 9-BB Dyes and Their Gels, PHEC Complexes	101
J. Olivares and V. Miras	
Low Dimensional Solids and Molecular Crystals	
Refractive Birefringence as a Function of Aging Temperature for Polydimethylsiloxane Networks grafted by Polystyrene Hexamethyl Polysiloxane Matrix	119
Manfred J. Peter	

Molecular Crystals and Liquid Crystals

Publication details, including instructions for authors and subscription information:

<http://www.informaworld.com/smpp/title~content=t713644168>

Synthesis, Properties and Applications of Conducting Polymer Nano-Objects

C. A. Barbero^a; D. F. Acevedo^a; E. Yslas^a; M. Broglia^a; D. O. Peralta^a; E. Frontera^a; R. Rivero^a; C. R. Rivarola^a; M. Bertuzzi^a; V. Rivarola^a; M. C. Miras^a

^a Programa de Materiales Avanzados, Universidad Nacional de Rio Cuarto, Rio Cuarto, Argentina

First published on: 28 May 2010

To cite this Article Barbero, C. A. , Acevedo, D. F. , Yslas, E. , Broglia, M. , Peralta, D. O. , Frontera, E. , Rivero, R. , Rivarola, C. R. , Bertuzzi, M. , Rivarola, V. and Miras, M. C.(2010) 'Synthesis, Properties and Applications of Conducting Polymer Nano-Objects', *Molecular Crystals and Liquid Crystals*, 521: 1, 214 – 228

To link to this Article: DOI: 10.1080/15421401003720074

URL: <http://dx.doi.org/10.1080/15421401003720074>

PLEASE SCROLL DOWN FOR ARTICLE

Full terms and conditions of use: <http://www.informaworld.com/terms-and-conditions-of-access.pdf>

This article may be used for research, teaching and private study purposes. Any substantial or systematic reproduction, re-distribution, re-selling, loan or sub-licensing, systematic supply or distribution in any form to anyone is expressly forbidden.

The publisher does not give any warranty express or implied or make any representation that the contents will be complete or accurate or up to date. The accuracy of any instructions, formulae and drug doses should be independently verified with primary sources. The publisher shall not be liable for any loss, actions, claims, proceedings, demand or costs or damages whatsoever or howsoever caused arising directly or indirectly in connection with or arising out of the use of this material.

Synthesis, Properties and Applications of Conducting Polymer Nano-Objects

C. A. BARBERO, D. F. ACEVEDO, E. YSLAS,
M. BROGLIA, D. O. PERALTA, E. FRONTERA,
R. RIVERO, C. R. RIVAROLA, M. BERTUZZI,
V. RIVAROLA, AND M. C. MIRAS

Programa de Materiales Avanzados, Universidad Nacional de Rio
Cuarto, Rio Cuarto, Argentina

Two different approaches are used to produce conducting polymer nano-objects. One is a “top-down” approach which involves laser ablation of conducting polymer films using laser light interference patterns (direct laser interference patterning, DLIP) to produce various surface shapes, including nanowires and nanodots. Polyaniline (PANI) and polypyrrole (PPy) nanostructures could be easily produced by ablation of films, previously formed by in-situ polymerization of the aromatic monomers. The other is a “bottom-up” approach involving the controlled nucleation and growth during monomer polymerization. This is achieved by performing the polymerization at the interface of two immiscible solvents. Both kinds of nanomaterials are characterized using dynamic light scattering, TEM, EDAX, FTIR, UV-vis and fluorescence spectroscopy. The structures are studied by SEM-FIB, optical and fluorescence microscopy along with water contact angle. It is shown that nanometric sized structures can be made by both methods. The chemical structures are quite similar or identical to that of the bulk polymer. While PANI nanofibers are dispersed in acid media, due to the surface charge related with chain protonation, they agglomerate in neutral media. In the interest of biological applications, different soluble polymers are used to help disperse the nanofibers at neutral pH. Both the dispersing agent and PANI nanofibers have to be innocuous to biological cells and higher organisms, like frog larvae. The successful intake of PANI nanofibers into cancer line cells and frog larvae prompts its application as NIR radiation absorbers in photothermal or photoacoustic tumor therapy and/or tomography.

Keywords Nanofibers; polyaniline; polypyrrole

Introduction

Nano-objects comprise a variety of physical species including stand alone nanoparticles, carbon nanotubes, surface patterns and self assembled multilayers [1]. While stand alone nano-objects are usually made by non deterministic “bottom-up” methods, such as nucleation and growth of metal colloids [2],

Address correspondence to C. A. Barbero, Programa de Materiales Avanzados, Universidad Nacional de Rio Cuarto, ruta 8, km 601, Rio Cuarto 5800, Argentina. Tel.: 0054 358 4676157; Fax: 0054 358 4676233; E-mail: cbarbero@exa.unrc.edu.ar

material patterns on surfaces are usually made by deterministic “top-down” method such as photolithography [3]. While it is customary to compare both approaches, they can be used as alternative or even as complementary ways to produce the desired nanostructure. In the present communication we describe the use of a top-down method: direct laser interference patterning (DLIP) to produce conducting polymer nanostructures. On the other hand we describe the synthesis of conducting polymer nanofibers by the method of nucleation and growth at liquid/liquid interfaces. Intrinsically conducting polymers (ICPs*) are interesting materials for technological applications. ICPs are essentially molecular objects, where the properties are independent on the size of the material, as far as one molecule is present [4]. This is unlike metal or semiconductors where clear size dependence of the properties is observed [5]. Such property could be an advantage to design nanometric systems using CP because bulk properties could be used at the design stage. However, it is clear that both intrachain electron delocalization and interchain charge hopping, which are relevant to the electronic properties, depend on the size and maybe shape of the material. Therefore, synthesizing CP nano-objects could render materials with novel properties. On the other hand, small objects are easily dispersed, have a high surface/volume ratio and mass transport is faster than in bulk counterparts [6].

Experimental

All reagents used are of analytical quality.

Film Formation

To assure adherence of the conducting polymer films, the surface of the PP or PE films oxidized by immersion in sulfochromic mixture during 15 min at ambient temperature. The oxidation renders the surfaces hydrophilic. Polyaniline films were produced onto PP, PE or PET by immersion of the polymer film in a polymerization solution which is 0.1 M in aniline, 1 M in HCl. To polymerize, an equimolar amount of ammonium persulfate is added. The reaction is carried out at below 5°C during 1 h. After the polymerization is finished, the film is washed with 1 M HCl, water and dried with a nitrogen stream [7]. Polypyrrole films are produced using similar experimental conditions [8].

Laser Interference Experiments

A high-power pulsed Nd:YAG laser (Quanta-Ray PRO 290, Spectra Physics) with a wavelength of 266 nm was used for the laser interference experiments. The pulse duration was 10 ns and only 1 laser pulse was used in each experiment. To obtain the line-like periodic patterns, the fundamental laser beam was split into two sub-beams and guided by mirrors to interfere on the sample surface. The samples were irradiated with laser fluences up to ca. 500 mJ cm⁻². All experiments were conducted in air at normal conditions of pressure and temperature.

*The term is used to distinguish from polymer based composites which contain another conducting material (e.g., carbon) which renders the composite conductive extrinsically.

Synthesis of Polyaniline Nanofibers by Interfacial Polymerization

24 mmols of aniline were dissolved in chloroform (75 ml). Ammonium peroxydisulfate (6mmoles) was dissolved in 75 ml of 0.8 M hydrochloric acid. The two solutions are then carefully transferred to a closed flask generating an interface. The monomer diffuses into the aqueous phase, where it is oxidized and polymerizes. All the reactions are performed in the dark. After 24 hours, the entire water phase is filled homogeneously with dark-green polyaniline, while the organic layer (chloroform) appears red-orange from by products. The aqueous phase is then collected and the remaining reactants and by-products are removed by dialysis, 4 days with deionized water and then 4 days with phosphate buffer solution (pH = 7.4).

Derivatization with Dansyl Chloride

Polyaniline nanofibers obtained by interfacial polymerization (pH = 1) were dialyzed against 1000 ml of PBS buffer solution (pH = 7.4) during 4 days and stored at -20°C until the time of derivatization. One ml of saturated sodium carbonate solution (pH = 9.5) and 1 ml of dansyl chloride (20 mg/ml in acetone) were then added to the tube containing 1 ml of the sample. The tube was capped, vortexed and incubated in a water bath at 60°C . After 60 min, 1 ml of a proline solution (100 mg/ml) was added to the reaction mixture to react with excess dansyl chloride. Following additional 30 min incubation, acetone was evaporated from the tube in a vacuum pump. The dansylated nanofibers are suspended on PBS solution and dialyzed against PBS by 4 days. Later, they are dialyzed for 4 days with sterile PBS solution and stored at -20°C . A pH of 9.5 is optimal for the dansylation of the unprotonated amine groups. While the nanofibers are tagged by the dansyl, they precipitate at pH 7. To avoid that, we developed a novel method involving wrapping the nanofiber with a soluble polyaniline chain as it was found to be effective with carbon nanotubes. The soluble polyanilines were synthesized as described before [9].

Characterization

Fourier transform infrared spectra (FTIR) of the polymers in the transmission mode were obtained in KBr pellets using a Bruker Tensor 27 spectrometer with a 4 cm^{-1} resolution. UV-visible spectra were measured using a HP-8452A diode array spectrometer. The size of dispersed PANI nanofibers were determined by dynamic light scattering (DLS, Malvern 4700 with goniometer and 7132 correlator) with an argon-ion laser operating at 488 nm. All measurements were made at the scattering angle of 90° . The fluorescence measurements were made in a Spex Fluoromax fluorometer using an excitation wavelength of 375 nm. All samples were imaged with a high-resolution scanning electron microscope (SEM) equipped with a field emission gun (FEI) Strata DB 235 at 5 kV acceleration voltage. The depth and period of the micropatterns were characterized using a White Light Interferometer (New View 200 3-D Imaging Surface Structure Analyzer, Zygo Corporation, USA). A computer controlled microscope Intel QX3 was used for measurement of contact angle by setting flat polymer pieces on a manually controlled tilt table, illuminating from behind with a white led source

and recording, with the microscope in horizontal position, the shape of water drops (3 μ l) standing still on the surface using a 60X objective. The pictures were analyzed using "Drop Analysis" software [10]. Fluorescence microscopy was performed in a Axiophot microscope (Zeiss, Germany) using a color camera (Axiocam, Zeiss, Germany) driven by Axiovision 4.3 software. The excitation and emission filters used were BP 436 FT and 460 LP 470 (Zeiss, Germany), respectively. Optical micrographs were taken using an Arcano XF125 optical microscope with a Motic 1000 1.3 MP digital camera linked to a PC using a USB port and driven by Motic 2000 Imaging software.

Biological Materials and Tests

The cell line used is the MCF-7c3 human breast cancer cells. The cells are maintained at 37°C in minimal essential media (MEM), with glutamine (1%) and supplemented with 7% of bovine fetal serum and gentamicine (30 mg/ml). MTT (3-(4,5-Dimethylthiazol-2-yl)-2,5-diphenyltetrazolium bromide) is reduced to purple formazan in living cells [11]. An acidified ethanol solution is added to dissolve the insoluble purple formazan product into a colored solution. The absorbance of the solution is quantified at a 550 nm. It was checked that PANI nanofibers does not absorb the formazan, as it happens with carbon nanotubes [12], giving false negatives.

Results and Discussion

Top-down Fabrication: Direct Laser Interference Patterning

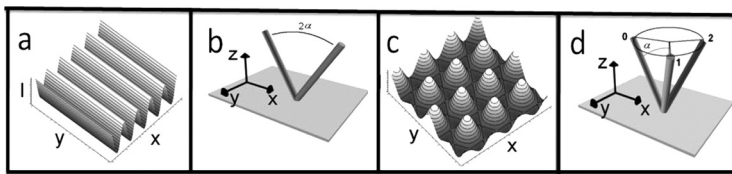
Direct laser interference patterning (DLIP) is a lithographic technique based on material ablation by a light pattern made with an intense laser beam [13]. The pattern is produced by interference of two or more laser beams (Scheme 1A). For 2-beam interference, the fringe-to-fringe spacing or period is given by

$$P = (\lambda/2) / \sin(\theta/2) \quad (1)$$

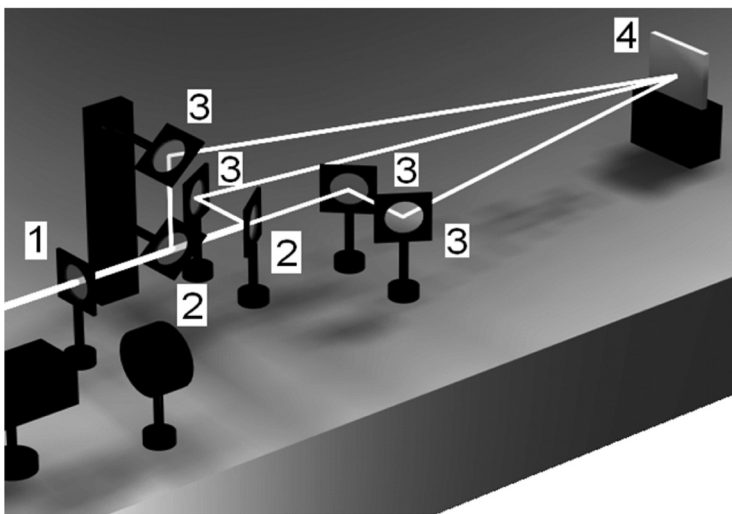
where λ is the wavelength and θ is the angle between the two interfering beams. The minimum period achievable is then half the wavelength. By using a 3-beam interference, arrays with hexagonal symmetry can be generated, while with 4 beams, arrays with rectangular symmetry are generated. Hence, by superimposing different beam combinations, different patterns are made possible. While there are different ways to create the interference, the usual way involves the division in amplitude using beam splitters (Scheme 1B).

It is possible to use very fast (picosecond or femtosecond) lasers but less expensive nanosecond lasers could also be used to the purpose. An essential condition is that the material to be patterned absorbs strongly light at the wavelength of the laser line. The commonly used Nd-Yag laser has a fundamental wavelength of 1064 nm which can be doubled (532 nm), tripled (266 nm) or mixed (355 nm).

To ablate conventional polymers (e.g., PMMA) it is necessary to include a dye [14] or copolymerize with an absorbing monomer unit [15]. However, due to the extended conjugation in its structure, conducting polymer absorbs both in the NIR (1064 nm), the UV (266 and 366 nm) and even the visible range (532 nm). Therefore are highly amenable to DLIP patterning.



(A)



(B)

Scheme 1. (A) Two and three-laser beams Interference patterns: (a) Line-type pattern with its correspondent two-laser beam; (b) configuration; (c) Dot-type pattern with its correspondent three-laser beam; (d) symmetrical configuration. The pattern is produced by interference of two or more laser beams; (B) Experimental setup for three-laser beam interference experiments: (1) Lens; (2) Mirror; (3) Beam-splitter; (4) Sample.

Another parameter is the thermal or chemical stability since highly stable materials could be difficult to ablate. Since the power density in nanosecond lasers is lower than in picosecond or femtosecond lasers, a less stable material is required. It is well known that typical conducting polymers (polyaniline, polypyrrole, polythiophene) decompose at temperatures below 200°C [16,17]. While it is possible to ablate bulk conducting polymers [18], it is easier to support the polymer as a film on a transparent substrate. This is easily done by depositing a thin film of the ICP by in-situ polymerization [19]. In the case of polyaniline, polyimide, polycarbonate, polyethylene, polypropylene, Indium doped tin oxide glass (ITO) or borosilicate glass were used as substrata. Clear patterning can be obtained by DLIP processing of the supported ICP films (Fig. 1) [20].

The thickness of the nanowires can be tailored by the period of the interference maxima and the fluence of the laser. The later effect is due to the fact that the light pattern has a sinusoidal shape but only radiation above a threshold is effective to produce ablation (Scheme 2).

In that way, the resistance of the nanowires can be easily tuned [21]. Since the polymer nanowires has the same chemical properties than bulk polyaniline,

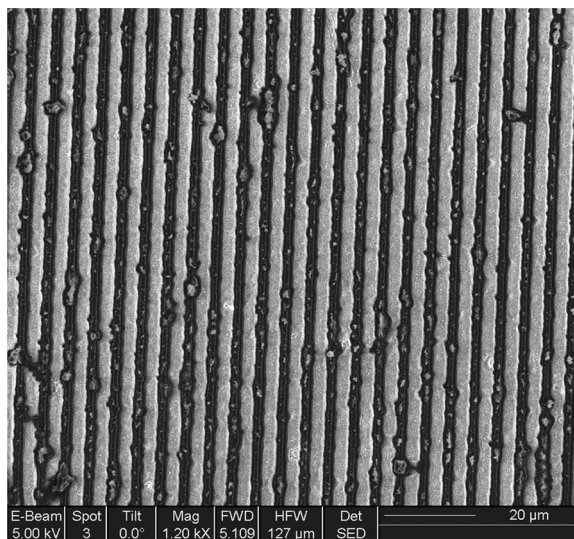
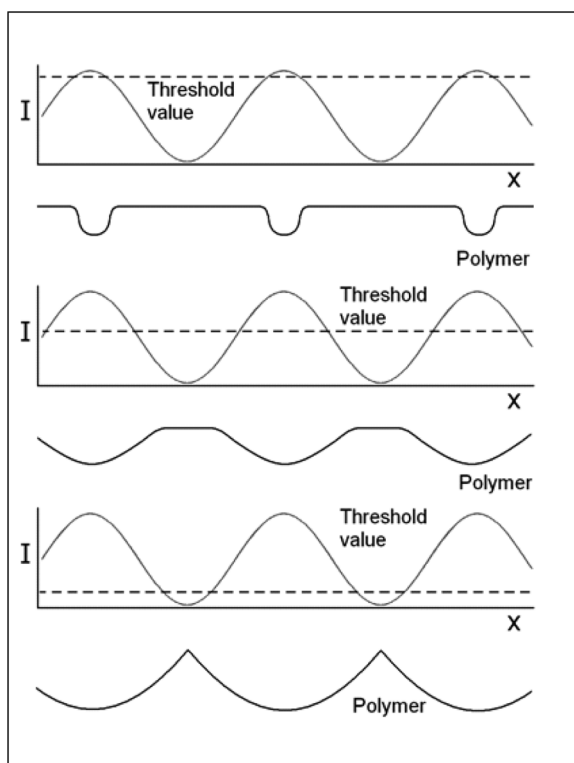


Figure 1. SEM micrograph of PANI/PI structured by DLIP.



Scheme 2. Relationship between the threshold values for ablation with the shape of the structure formed.

it is possible to build electronic sensors of vapors or solutes. Additionally, the response rate could be much higher than of bulk counterparts as it has been shown for sensors built with conducting polymer nanofibers [22]. Depending on the light absorption of the substrate polymer, it could also be ablated together with PANI as it is shown in a SEM micrograph of a FIB cross section of PANI/PI (Fig. 2).

The conducting polymer could be ablated even more easily when it is deposited on inorganic materials, which have a higher thermal stability. In Figure 3 it is shown the line pattern produced by DLIP ablation of a PANI film deposited on Indium doped Tin Oxide (ITO). Given the large difference of thermal stability, clear patterns are produced. Since ITO is conductive, either the PANI film can be produced electrochemically or the pattern can be used as structured electrode in electrochemical systems, such as sensors.

While polyaniline is a conducting polymer useful in many applications, its conductivity is very low at biological pH (above 6) because the conducting form becomes deprotonated [23] at pH 4–5. On the other hand, polypyrrole (PPy) is conductive at physiological pH because the deprotonation causes a minor effect on the conductivity. DLIP ablation of PPy (deposited onto PP) renders clear line or point patterns (Fig. 4).

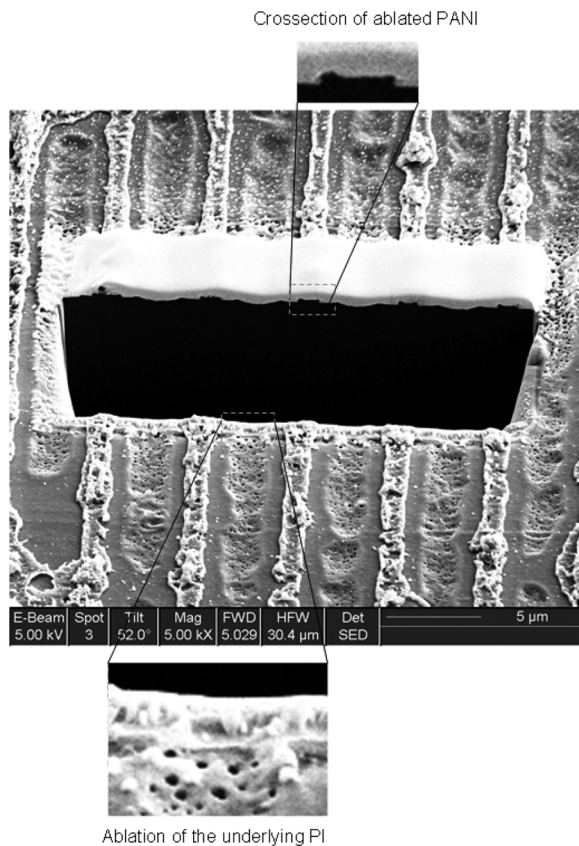


Figure 2. SEM micrograph of a FIB cross section on a PANI/PI film structured using DLIP.

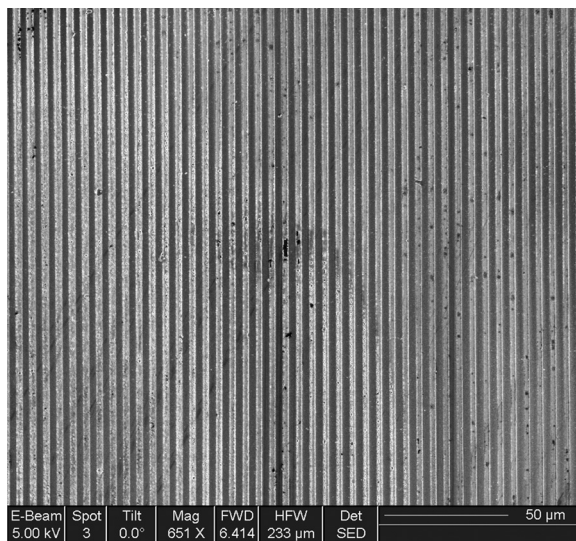


Figure 3. DLIP Pattern of PANI deposited on ITO.

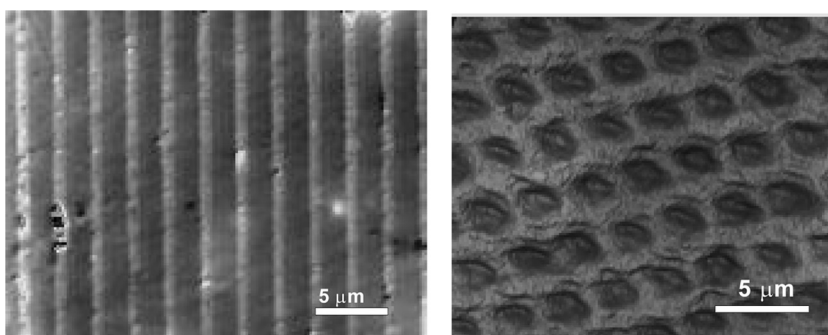


Figure 4. White light interferogram image of PPy/PP structured by DLIP using two beams (left) or three beams (right).

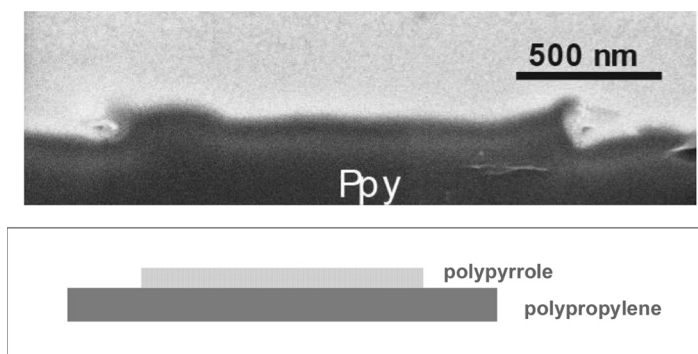


Figure 5. SEM micrograph of a FIB cross section of a PPy/PP structured film. Below it can be seen a scheme of the structured multilayer.

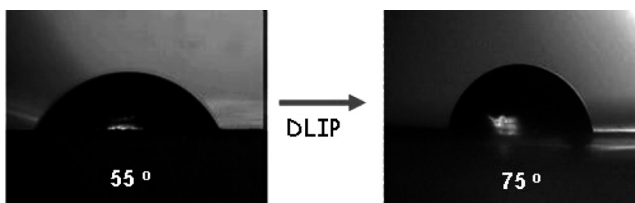


Figure 6. Contact angle of water drops deposited onto flat (left) and DLIP line structured (right) PPy films on PP.

An examination of the line pattern cross section, made with FIB, (Fig. 5) reveals that only PPy is ablated while the substrate polymer (PP) remains unaltered. It is likely that the energy deposited by the laser light on the PPy layer is not enough to decompose the more stable PP. On the other hand, at the wavelength used (355 nm), the absorption by PP is negligible.

Previously, it has been shown that DLIP patterning of acrylate based polymers changes the wettability of polymer surfaces due to the creation of novel air/solid/liquid interfaces below the water drop [24]. It is likely that structuring also alters the wettability of PPy. In Figure 6 are shown the water drops standing on top of flat and structured PPy. As expected, the structured surface is more hydrophobic (water contact angle of 75°) than the flat one (water contact angle of 55°). This is likely due to the formation of air pockets below the water drops as proposed before [25].

The same behavior is observed in the case of PANI deposited on PP (Fig. 7).

It seems that the topographic effect on the wetting can be achieved with different conducting polymers. Since it is known that wettability of conducting polymers can be controlled by changing its redox state, [26,27] the additional hydrophobic effect due to the structuring could help to design better electrically driven wetting actuators.

Bottom-up Fabrication: Interfacial Polymerization of Nanofibers

Polyaniline nanofibers are small objects which are suitable as multifunction vectors for insertion of bioactive principles into living cells. Additionally, the optical properties of the fibers could be used with advantage in Near Infrared (NIR) photothermal therapy and/or tomography [28]. Polyaniline has a broad absorption band, due to free carrier absorption, with a maximum at ca. 800 nm in the NIR range. Living



Figure 7. Contact angle of water drops deposited onto flat (left) and DLIP line structured (right) PANI films on PP.

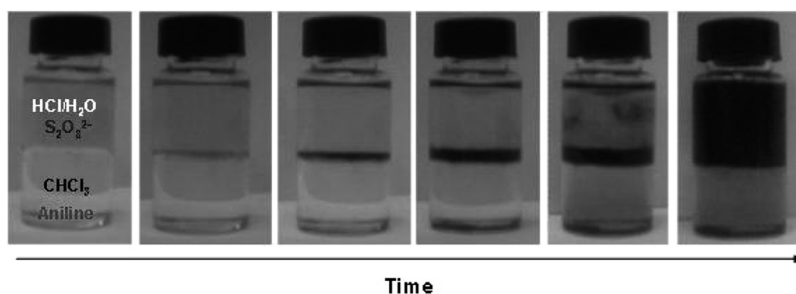


Figure 8. Snapshots showing the interfacial polymerization of aniline. The reaction times are 0, 60, 90, 120, 180, 270, and 360 seconds. The top layer is an aqueous solution of acid and oxidant, the bottom layer is aniline dissolved in chloroform.

tissue absorbs little light between 700 and 1200 nm. Therefore, light in this region could penetrate several centimeters to be absorbed by a suitable susceptor, such as polyaniline.

Polyaniline nanofibers can be easily synthesized by interfacial polymerization [29] (Fig. 8). As it can be seen, the monomer diffuses from the lower CHCl_3 layer towards the upper aqueous layer where it is oxidized by the persulfate ion at the interface. The low concentration of aniline at the interface assures that a large number of nuclei is formed and PANI nanofibers grow in the aqueous solution.

The PANI nanofibers seem to be flat and of irregular size and shape (Fig. 9).

The size of the fibers can be controlled by changing the counterion present during polymerization. In the case of perchlorate, a mean value of ca. 600 nm is obtained (Fig. 10). Obviously this is not the diameter or length of the nanofiber, but the diameter of the revolution sphere described by the rod-like nanofiber in solution. The nanofibers are dispersed evenly in the solution, as it can be seen from the dynamic light scattering measurement (Fig. 10).

While PANI nanofibers form a stable suspension in acid media, due to the repulsion of charges built up on the fibers by protonation, they precipitate at

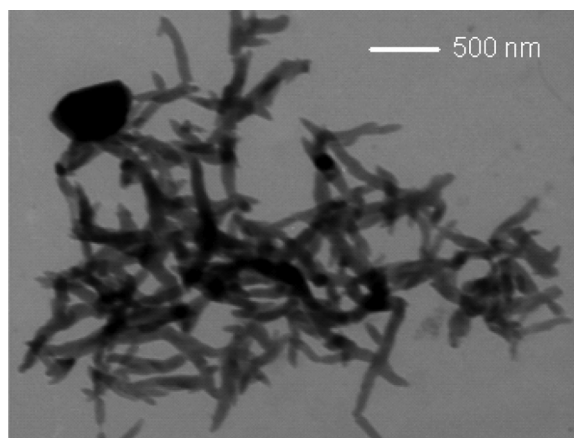


Figure 9. TEM micrographs of PANI nanofibers.

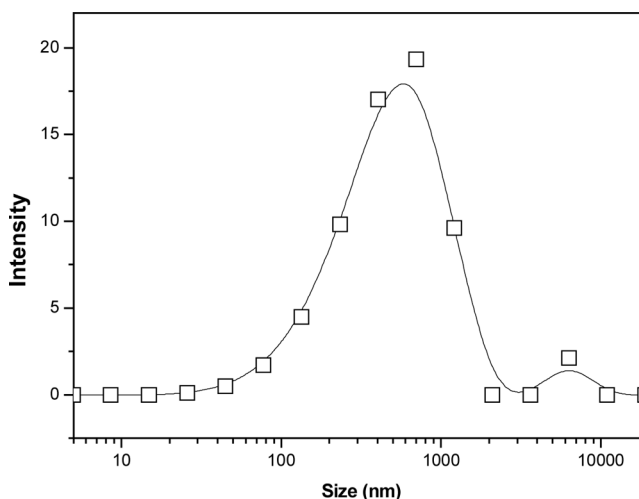


Figure 10. Size distribution of dispersed PANI nanofibers obtained by Dynamic light scattering.

physiological pH, at which the fiber surface is deprotonated. To overcome that, we use a soluble polyaniline, functionalized by reaction of diazonium ion with plain polyaniline [30], as a non covalent solubilizing agent [31]. The UV-visible spectra of the nanofiber dispersion (Fig. 11) changes with pH in a similar way to bulk polymer films [32]. For our purposes it is relevant that at both pH there is a clear absorption in the NIR range (800–1100 nm).

To follow the intake of PANI nanofibers into the cells, the surface of the nanofiber is stained with a Dansyl fluorescent tag. The fluorescence spectra show a clear luminescence (Fig. 12).

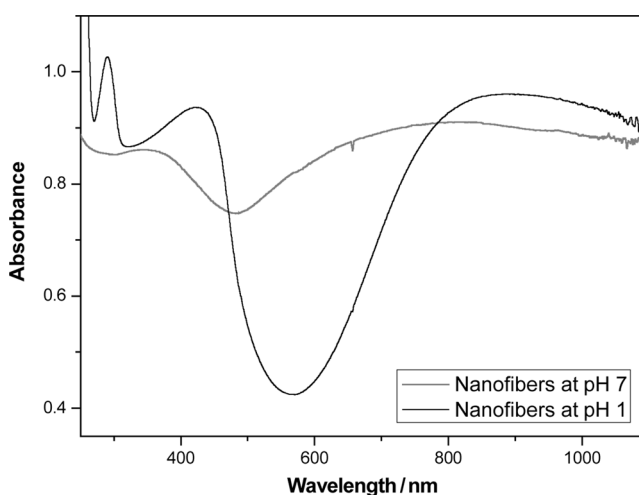


Figure 11. UV-visible spectra of PANI nanofibers at different pH, dispersed using a soluble polyaniline.

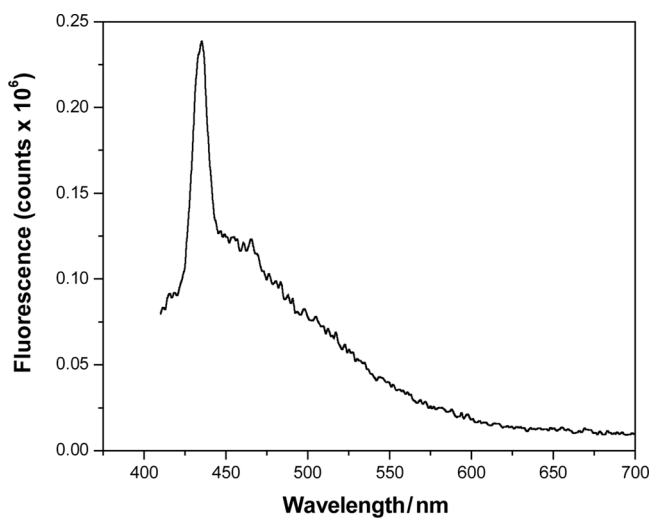


Figure 12. Emission spectra of polyaniline nanofibers ($\lambda_{\text{exc}} = 350$ nm).

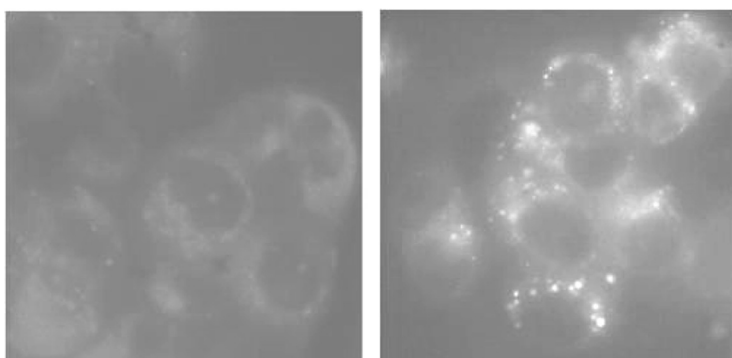


Figure 13. Fluorescent microscopy images of tumor cells with incorporated dansylated nanofibers (left image = 435/546 nm, right image 345/425 nm).

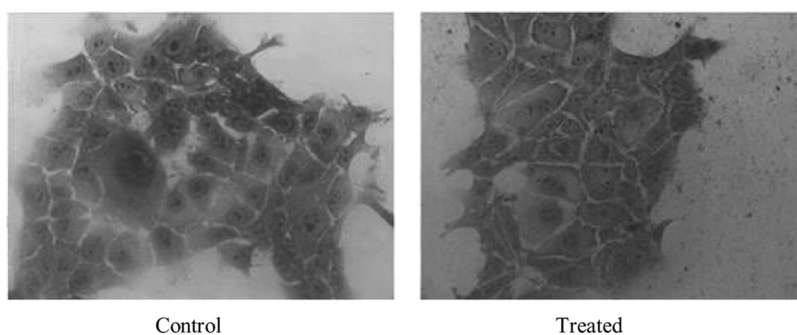


Figure 14. Optical micrographs of fibroblasts exposed to PANI nanofiber dispersion (right) compared with control cells (left). The morphology of the cells seems unaltered.

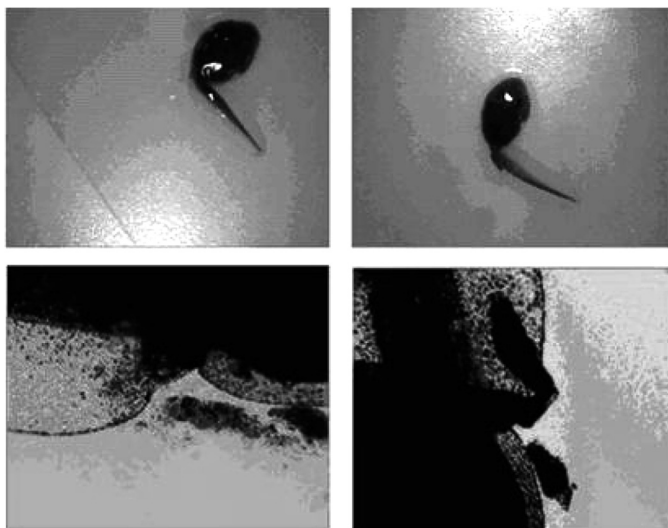


Figure 15. Optical micrographs of *bufo arenarum* larvae grown with PANI nanofibers as only carbon source.

Then immobilized cells (MCF-7, Human Breast Adenocarcinoma Cell Line) are incubated (3 and 6 hrs) in a medium Dulbecco's Modified Eagle's Medium (DMEM) containing dispersed nanofibers dissolved in PBS. It is found that, below a concentration threshold (100 ng/ml), PANI nanofibers are innocuous to the cells in the dark. The tagged nanofibers are easily detected inside the cytoplasm by fluorescence microscopy, indicating that they are inserted into the cells. After 2 hrs, the nanofibers translocate into the cell nucleus. Fluorescence microscopy shows clearly the intake of nanofibers by the cells (Fig. 13).

Biological cells exposed to PANI nanofibers during 24 hrs, does not show significant morphological changes, in comparison with the control, or cell death (Fig. 14).

MTT tests show cell viability upon exposure. To test toxicity to higher organisms, the PANI nanofibers were fed to frog larvae upon a 14 days growth cycle. The larvae show normal growth without undue morphology changes (Fig. 15).

Using a 808 nm, 2 W GaAs laser a temperature increase of 8–10 degrees was found. Such changes are enough to promote the apoptosis of tumor cells.

Conclusions

It is possible to fabricate conducting polymer nanostructures both by “top-down” and “bottom-up” approaches. Direct laser interference patterning is a suitable method to create conducting polymer nanostructures from supported polymer films. Both polyaniline and polypyrrole can be patterned. The films can be deposited and structured on conventional polymers or inorganic materials. The structuring makes the polymer surface more hydrophobic. Polyaniline nanofibers can be easily produced by interfacial polymerization of aniline. The nanofibers can be dispersed in physiological pH solutions using soluble polyanilines or poly(vinylpyrrolidone) as stabilizers. The nanofibers can be tagged using fluorescent dyes. In that way, it

is shown that PANI nanofibers are internalized into living cells without noticeable cytotoxicity. The nanofibers are not theratogenic to frog larvae. PANI nanofiber dispersion can be heated up to 8–10 centigrade above ambient by illumination with a 2 W NIR (808 nm) laser during 1 min.

Acknowledgments

The authors acknowledge the support of CONICET, FONCYT, John Simon Guggenheim Foundation and SECYT-UNRC. A. Lasagni and F. Mücklich are gratefully thanked for the SEM-FIB and WLI measurements. C. Barbero, D.F. Acevedo, C.R. Rivarola, E. Yslas, and V. Rivarola are permanent research fellows of CONICET.

References

- [1] Ozin, G.A. & Arsenault, A. C. (2005). *Nanochemistry*, The Royal Society of Chemistry: UK.
- [2] (a) Schmid, G. (2004). *Nanoparticles: From Theory to Application*, Wiley-VCH: Weinheim; (b) Hans Kuzmany, Mehring, M., Fink, J., & Roth, S. (2008). *Electronic Properties of Synthetic Nanostructures*, Springer-Verlag: New York.
- [3] Guo, Z. & Tan, L. (2009). *Fundamentals and Applications of Nanomaterials*, Artech House, Inc.: New York.
- [4] Roth, S. (1995). *One-Dimensional Metals: Physics and Materials Science*, John Wiley & Sons: New York.
- [5] Hawrylak, P. & Wojs, A. (1998). *Quantum Dots*, Springer: Heidelberg.
- [6] Virji, S., Jiaying, H., Kaner, R. B., & Weiller, B. H. (2004). *Nanoletters*, 4, 491.
- [7] Stejskal, J. & Gilbert, R. G. (2002). *Pure Appl. Chem.*, 74, 857.
- [8] Lee, J. Y., Song, K. T., Kim, S. Y., Kim, Y. C., Kim, D. Y., & Kim, C. Y. (1997). *Synth. Metals*, 84, 137.
- [9] Acevedo, D. F., Salavagione, H. J., Miras, M. C., & Barbero, C. A. (2005). *J. Braz. Chem. Soc.*, 16, 259.
- [10] Biomedical Imaging Group, download algoritm. <http://bigwww.epfl.ch/demo/dropanalysis/>
- [11] Mosmann, T. (1983). *Journal of immunological method*, 65, 55.
- [12] Belyanskaya, L., Manser, P., Spohn, P., Bruinink, A., & Wick, P. (2007). *Carbon*, 45, 2643.
- [13] Lasagni, A., Holzapfel, C., Weirich, T., & Mücklich, F. (2007). *Applied Surface Science*, 253, 8070.
- [14] Lippert, Th., Wokaun, A., Stebani, J., Nuyken, O., & Ihlemann, J. (1993). *Die Angewandte Makromolekulare Chemie*, 213, 127.
- [15] Acevedo, D. F., Lasagni, A. F., Cornejo, M., Politano, M., Barbero, C., & Mücklich, F. (2009). *Langmuir*, 25, 9624.
- [16] Rannou, P. & Nechtschein, M. (1997). *Synthetic Metals*, 84, 755.
- [17] Cheah, K., Forsyth, M., Truong, V.-T., & Olsson, C. (1997). *Synthetic Metals*, 84, 829.
- [18] Raimondi, F., Wambach, J., Wei, J., & Wokaun, A. (1999). *Appl. Phys. A*, 69, S291.
- [19] Stejskal, J., Sapurina, I., Proke, J., & Zemek, J. (1999). *Synthetic Metals*, 105, 195.
- [20] Acevedo, D. F., Lasagni, A., Barbero, C. A., & Mücklich, F. (2007). *Advanced Materials*, 19, 1272.
- [21] Lasagnil, A. F., Acevedo, D. F., Barbero, C. A., & Mücklich, F. (2008). *Appl. Phys. A*, 91, 369.
- [22] Huang, J., Virji, S., Weiller, B. H., & Kaner, R. B. (2004). *Chem. Eur. J.*, 10, 1314.
- [23] Kang, E. T., Neoh, K. G., & Tan, K. L. (1995). *Synthetic Metals*, 68, 141.

- [24] Acevedo, D. F., Martinez, G., Toledo Arana, J., Yslas, E. I., Mucklich, F., Barbero, C., & Salavagione, H. J. (2009). *J. Phys. Chem. B*, *113*, 14661.
- [25] Lin, F. (2008). *Langmuir*, *24*, 4114.
- [26] Isaksson, J., Robinson, N. D., & Berggren, M. (2006). *Thin Solid Films*, *515*, 2003.
- [27] Robinson, L., Isaksson, J., Robinson, N. D., & Berggren, M. (2006). *Surface Science*, *600*, L148.
- [28] Huang, X., El-Sayed, I. H., Qian, W., & El-Sayed, M. A. (2006). *J. Am. Chem. Soc.*, *128*, 2115.
- [29] Li, D. & Kaner, R. B. (2006). *J. Am. Chem. Soc.*, *128*, 968.
- [30] Acevedo, D. F., Miras, M. C., & Barbero, C. A. (2005). *J. Combin. Chem.*, *7*, 513.
- [31] Acevedo, D. F., Balach, J., Rivarola, C., Miras, M. C., & Barbero, C. A. (2006). *Faraday Discussions*, *131*, 352.
- [32] Huang, W. S. & MacDiarmid, A. G. (1993). *Polymer*, *34*, 1833.